Article

Determination of Dipyridamole Using a MIP-Modified Disposable Pencil Graphite Electrode

Daniel Preda [1], Maria Lorena Jinga [2], Iulia Gabriela David [2,*] and Gabriel Lucian Radu [3,*]

[1] Doctoral School of Chemical Engineering and Biotechnologies, University Politehnica of Bucharest, Gheorghe Polizu Street 1-7, District 1, 011061 Bucharest, Romania; daniel.preda1208@stud.chimie.upb.ro

[2] Department of Analytical Chemistry and Physical Chemistry, Faculty of Chemistry, University of Bucharest, Panduri Av. 90-92, District 5, 050663 Bucharest, Romania; maria.jinga@s.unibuc.ro

[3] National Institute of Biological Sciences, Centre of Bioanalysis, Splaiul Independentei 296, District 6, 060031 Bucharest, Romania

* Correspondence: gabrielaiulia.david@g.unibuc.ro (I.G.D.); lucian.radu@incdsb.ro (G.L.R.)

Abstract: A new method for the determination of the antiplatelet drug dipyridamole (DIP) in pharmaceuticals using a molecularly imprinted polymer (MIP)-modified pencil graphite electrode (PGE) is proposed. The modified electrode was prepared simply and rapidly by electropolymerization of caffeic acid (CA) in the presence of DIP and subsequent DIP extraction with ethanol, resulting in a cost-effective, eco-friendly disposable modified electrode (MIP_PGE). Several working conditions (monomer and template concentration, number of voltametric cycles, scan rate extraction time, and solvent) for the MIP_PGE preparation were optimized. The differential pulse voltammetric (DPV) oxidation signal of DIP obtained at MIP_PGE was 28% higher than that recorded at bare PGE. Cyclic voltammetry emphasized DIP irreversible, pH-dependent, diffusion-controlled oxidation at MIP_PGE. Differential pulse and adsorptive stripping voltammetry at MIP_PGE in phosphate buffer solution pH = 7.00 were applied for the drug quantitative determination in the range of 1.00×10^{-7}–1.00×10^{-5} and 1.00×10^{-8}–5.00×10^{-7} mol/L DIP, respectively. The obtained limits of detection were at the tens nanomolar level.

Keywords: dipyridamole; molecularly imprinted polymer; modified electrodes; electroanalysis; pencil graphite electrode; disposable electrode

1. Introduction

Dipyridamole (DIP), 2,6-bis-(diethanolamino)-4,8-dipiperinopyrimido [5,4-d] pyrimidine (Figure 1) is one of the most prescribed antithrombotic drugs administered orally. It was first introduced in 1959 as a coronary vasodilator and anti-anginal agent, and it was prescribed for myocardial infarction prevention, post-coronary angioplasty, and artery bypass surgery. It was demonstrated that, when it is administered in addition to aspirin, it can induce an augmentation of platelet-inhibiting action due to a pharmacokinetic interaction between them [1]. Unfortunately, despite this drug's benefits, it also shows some inconveniences, such as inducing coronary ischemia when it is administered intravenously, and some side effects, such as chest tightness, dizziness, abdominal pain, and headache [2].

On the other hand, some reports showed that DIP is used fraudulently in sports competitions as it has incredible effects on decreasing tiredness and improving efficiency [3]. Moreover, a recent study has proven that DIP is involved in SARS-CoV-2 replication in vitro suppression. According to some recent reports, this drug has also provided numerous advantages in patient therapy due to its antiviral activity against RNA viruses, promotion of mucosal healing, decreasing inflammation properties, and prevention of acute injury and progressive fibrosis of body organs [4]. DIP also has antioxidant activity when it behaves as an inhibitor of lipid peroxidation [5].
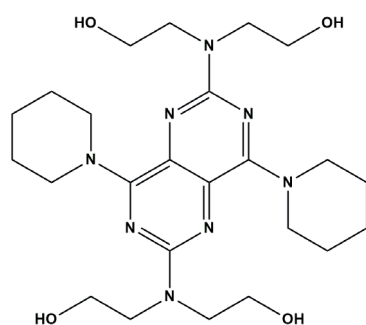
Figure 1. Structural formula of dipyridamole.

Overall, due to its impressive benefits, DIP determination in pharmaceuticals and various biological samples became really important. There are numerous analytical methods proposed for this drug quantification which encompass more conventional techniques, such as HPLC [6–10] and spectrophotometry [11,12]. Despite their advantages, these methods have also shown important limitations, such as the need for time-consuming preliminary procedures, such as extraction and concentration in organic solvents, that imply large volumes of samples and reagents, expensive equipment, and the necessity of specialized personnel, in the case of chromatographic methods. Polarography is no longer used due to mercury toxicity. Spectrophotometry and conductometry have low sensitivity and selectivity. On the other hand, methods, such as phosphorimetry [13], chemiluminescence [14], and fluorimetry [15], have shown the achievement of lower limits of detection and higher selectivity and sensitivity compared to other traditional detection methods of DIP.

In terms of analysis time and cost, the electrochemical methods are the most preferred by the researchers. These methods are simple, rapid, sensitive, and selective when using modified electrodes, thus possessing a big potential in DIP quantification [16–19]. A special category of materials employed for sensor surface modification in order to improve their performance characteristics is represented by molecularly imprinted polymers (MIPs). Those are polymers that contain cavities with the same shape and dimensions as the analyte(s) molecule(s), acting as selective recognition sites for the species of interest, which was used as a template molecule in the polymerization step and was removed afterward [20]. The aim of this study was to develop a cheap and disposable MIP-modified sensor for rapid and sensitive DIP determination. The literature presents two MIP-based electrodes for DIP determination [21,22], but the MIPs used there were prepared by applying a chemical procedure, which was more complicated, needed more time, and employed more reagents than the electropolymerization procedure used in this study. Despite the fact that the MIP_PGE fabrication reported in this paper was very simple and rapid, it did not involve expensive or toxic materials; the working electrode support was constituted by ordinary pencil leads, commonly used for writing; caffeic acid (CA) used as the monomer is a naturally occurring polyphenol, and the solvent used for the template extraction was ethanol.

2. Materials and Methods

2.1. Reagents and Solutions

DIP (dipyridamole, >98% TLC powder), CA (caffeic acid, 97.0%), glucose (Sigma-Aldrich, Darmstadt, Germany), urea (Sigma-Aldrich), thiamine hydrochloride (reagent grade $\geq$ 99%), ascorbic acid, aspirin (Sigma-Aldrich), EtOH (ethanol, $\geq$96% ACS reagent), $Na_2HPO_4 \times 2H_2O$ and KH_2PO_4 (p.a., ACS reagent), CH_3COOH ($\geq$99.7%, ACS reagent), NaOH (pellets), H_3BO_3 (1 g per tablet), H_3PO_4 (85 wt% in H_2O), were purchased from Sigma-Aldrich, and dipyridamole tablets (one tablet contained 25 mg of active principle (DIP), starch, lactose monohydrate, microcrystalline cellulose, povidone K30, talc, magnesium stearate, hypromellose, TiO_2, macrogol 6000 and sunset yellow) produced by S.C. Zentiva S.A. were bought from a local drug store.

Phosphate buffer solution (PBS) pH = 7.00 and Britton–Robinson buffer (BRB) solutions with pH values in the range of 1.81–11.00 were used as supporting electrolytes.

2.00×10^{-3} mol/L DIP and 1.00×10^{-2} mol/L CA stock solutions were daily fresh prepared in ethanol under sonication until complete dissolution and stored in the refrigerator when not used. More diluted DIP and CA working solutions were obtained from the corresponding stock solutions by proper (successive) dilutions with the appropriate amounts of supporting electrolyte solution. The 0.5-mm diameter Rotring pencil graphite leads acted as the active surfaces of the working electrodes. The pencil leads were purchased from a local bookstore.

2.2. Instrumentation

Electrochemical recordings were conducted using a conventional voltammetric cell comprising a Pt wire and an Ag/AgCl (3.00 M KCl) acting as auxiliary and reference electrodes, respectively, and a bare or MIP-modified PGE as a working electrode. The whole system was connected to a potentiostat/galvanostat Autolab PGSTAT 12 (Metrohm, Schiedam, the Netherlands) linked to a PC equipped with GPES 4.9. software used for the control of the potential applied to the working electrode, voltammogram recordings, and data acquisition and interpretation. The PGE with a surface area of 15.86 mm^2 (0.50 mm diameter and 1.00 cm height exposed to the analyzed solution) consisted of the HB-type graphite pencil leads prepared as previously described [23].

Electrochemical impedance (EIS) measurements were carried out with a PGSTAT302N potentiostat/galvanostat (Metrohm) equipped with a 3-electrode cell (Metrohm) controlled with Nova 1.11 software.

A Consort P901 Scientific Instrument pH/mV/°C-meter (Belgium) equipped with a combined pH-sensitive glass electrode was used for the measurements of the solutions' pH values.

2.3. Procedures

Electropolymerization of CA (monomer) in the presence of DIP (template) on the PGE surface was carried out potentiodynamically in PBS pH = 7.00 applying 5 potential cycles in the potential range from 0.000 to 2.000 V at a scan rate of 0.100 V/s. In order to obtain the MIP_PGE, the template (DIP) was removed from the poly (caffeic acid) (pCA) film deposited at the PGE by extraction for 2 h in ethanol (Scheme 1). The complete elimination of the DIP from the polymeric matrix was confirmed by the absence of the DIP characteristic oxidation signal recorded by DPV in the supporting electrolyte (PBS pH = 7.00). For comparison, a non-imprinted poly (caffeic acid) modified PGE (NIP_PGE) was prepared by CA polymerization in the absence of DIP using the same conditions as presented above.
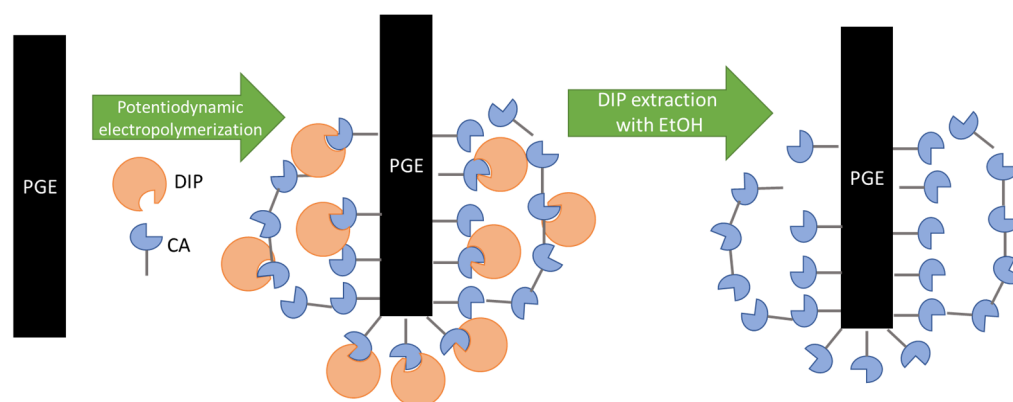
Scheme 1. Schematic representation of the steps involved in the preparation of the MIP_PGE.

Differential pulse voltammetric (DPV) curves were recorded at room temperature (25.0 ± 0.2 °C) under the following instrumental parameters: modulation amplitude 75 mV; step potential 4.94 mV; interval time 0.1 s; and modulation time 0.002 s.

The EIS measurements were performed in 1.00×10^{-3} mol/L ferro-ferricyanide in PBS pH = 7.00 in the frequency range of 0.1 Hz–10.0 kHz at a DC potential of 0.230 V. The results were represented as Nyquist plots and interpolated using Randles equivalent circuit. The experimental data of EIS were fitted with the classic Randles equivalent circuit, where Rs is the electrolyte resistance; Rct is the charge transfer resistance at the electrode interface; Q is the constant phase element related to the double layer capacitance, and W is the Warburg impedance used to simulate the mass-transport effects in solution bulk. Rct was used for the surface characterization.

Ten tablets of dipyridamole containing 25 mg active principle per tablet were weighed and crushed with a pestle in a mortar until a fine powder was obtained. Considering the DIP content of the tablets declared by the producer, the amount of this powder calculated to be necessary to obtain 50 mL of 1.00×10^{-3} mol/L DIP solution was dissolved in about 25 mL ethanol under 30 min sonication and then filtered directly in the volumetric flask. In order to avoid any analyte loss, the filter paper was rinsed three times with ethanol. The washing solutions were collected together with the filtrate in the same volumetric flask, which was finally brought to the mark with ethanol, resulting in 50 mL dipyridamole tablet solution, with the theoretical concentration of 1.00×10^{-3} mol/L DIP. The working solution (dipyridamole tablet sample solution) with a theoretical concentration of 1.00×10^{-6} mol/L DIP, situated in the linearity range of the developed method, was prepared right before being analyzed, by introducing 0.025 mL of the dipyridamole tablet solution into a 25 mL volumetric flask and diluting to the mark with PBS pH = 7.00. To minimize the matrix interferences, the standard addition method was applied to assess the dipyridamole tablet content, also taking into consideration the dilutions made. Thus, DIP oxidation peak heights (I_p) measured from the DPV curves recorded at the MIP_PGE for 10 mL of dipyridamole tablet sample solution before and after each of the 3 successive additions of 0.025 mL of 1.00×10^{-3} mol/L DIP stock solution were employed to construct the I_p (A) = f (C_{add}, mol/L) graph, where C_{add} represents the concentration of the added DIP into the analyzed solution. The regression equation was then used to calculate the DIP concentration from the dipyridamole tablet sample solution.

3. Results

3.1. Electropolymerization of Caffeic Acid in the Presence of Dipyridamole

In order to obtain the MIP_PGE, electropolymerization of CA (monomer) in the presence of DIP (template) in PBS pH = 7.00 (supporting electrolyte) at the PGE surface was carried out by applying five potential cycles between 0.000 and 2.000 V (Figure 2a). The NIP_PGE was prepared in the same conditions but in the absence of DIP (Figure 2b). In the direct scan of the first voltammetric cycle recorded for obtaining the MIP_PGE (Figure 2a), one can observe two anodic signals at cca. 0.300 V (peak a) and at cca. 0.500 V (peak b), respectively. Comparing the voltammograms recorded for the monomer–template mixture (Figure 2a) with those obtained for each individual component (Figure 2b,c), the peak situated at less positive potentials (peak a) can be attributed to the CA oxidation, while the signal from about 0.500 V (peak b) corresponded to DIP anodic process at cca. 0.300 V and cca. 0.500 V, respectively. During the reversed scan, even of the first cycle, a cathodic peak appeared at cca. 0.150 V (Figure 2a). Starting with the second scan, these two peaks decreased dramatically, the DIP signal (b) (Figure 2a,c) disappearing totally starting with the third scan, while peak (a) shifted toward less positive potentials (Figure 2a,b). Moreover, according to Nian Bing Le et al. [24], the signal from cca. 0.230 V can be attributed to the formation of the poly (caffeic acid) (pCA) film. On the other hand, peak (a) formed a redox couple with the cathodic one, which corresponded to the o-quinone/o-hydroquinone pair that sustained the formation of pCA film [25,26]. The enhancement of the currents of these two peaks with increasing cycle numbers suggested that a conducting polymer was generated at the electrode surface. A recent paper reported the formation of the pCA film at a carbon-based electrode (namely, a glassy carbon electrode) applying high voltages, and the existence of the polymeric film was confirmed by FTIR analysis [27].
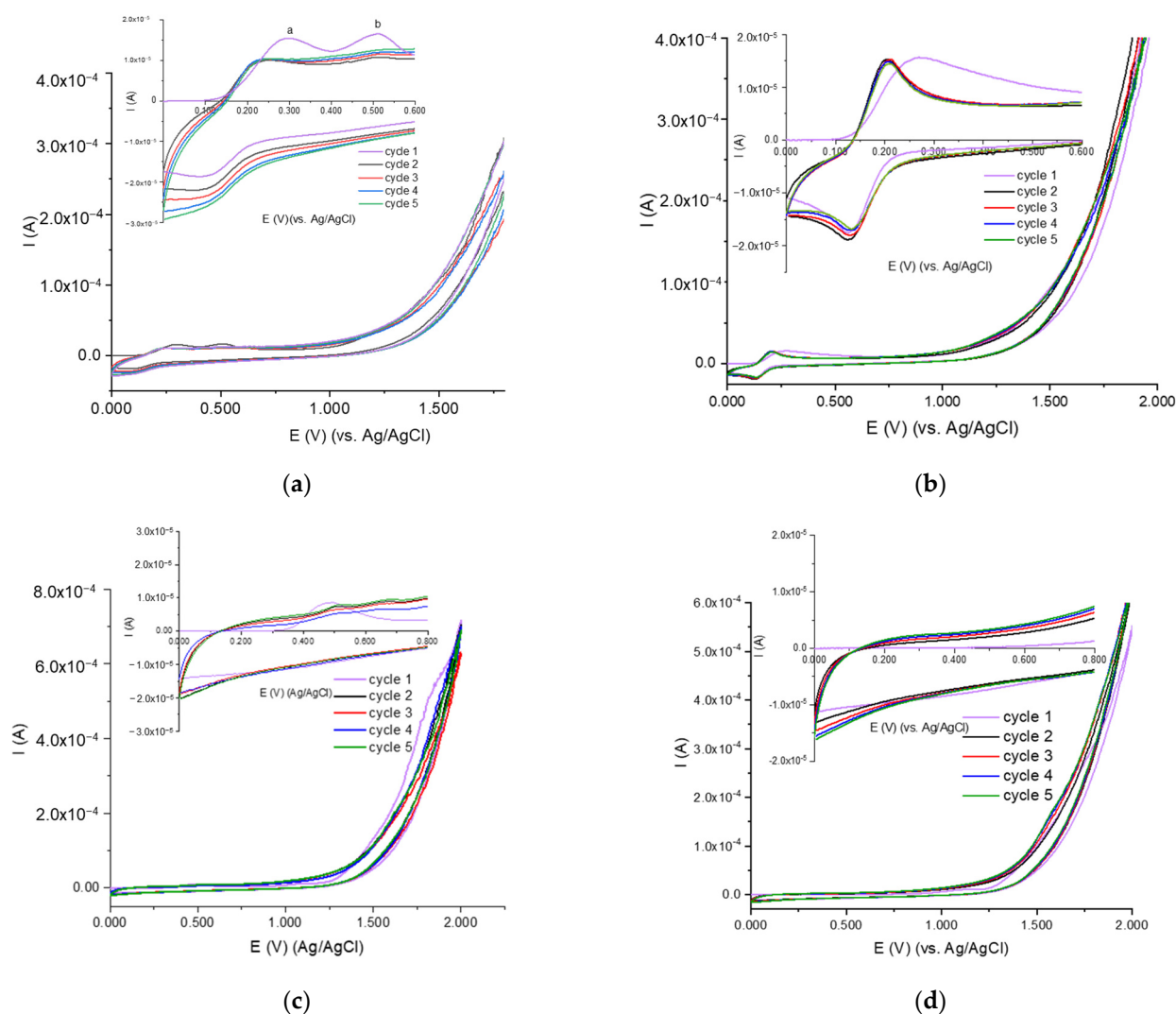
Figure 2. Repetitive cyclic voltammograms recorded at PGE for solutions of (**a**) 2.00×10^{-4} mol/L CA in the presence of 4.00×10^{-5} mol/L DIP in PBS pH = 7.00, (**b**) 2.00×10^{-4} mol/L CA in PBS pH = 7.00, (**c**) 4.00×10^{-5} mol/L DIP in PBS pH = 7.00, and (**d**) PBS pH = 7.00. Scan rate 0.100 V/s. Inset: enlarged section of the potential window where the CA and DIP signals were observed.

3.2. Optimization of the Experimental Conditions for the Electrochemical MIP Preparation

To obtain a MIP, two main stages must be completed, namely, (i) the monomer polymerization in the presence of the template and (ii) the removal of the embedded template from the polymeric matrix. Various parameters of these steps must be optimized in order to achieve the best voltammetric response of the MIP-modified electrode toward the analyte of interest.

3.2.1. Optimization of the Electropolymerization Conditions

- The influence of the monomer and template concentration

The monomer and template concentration in the polymerization mixture has an effect on the number of cavities and, thus, the recognition capacity of a MIP. Therefore, the influence of the monomer (CA) concentration in the polymerization solution on the DIP response at the MIP_PGE was investigated by comparing the DIP peak current (I_p) recorded by DPV in PBS pH = 7.00 at PGE modified with MIP films obtained by CV maintaining a fix template concentration (4.00×10^{-5} mol/L DIP) and different monomer concentrations comprised the range of 5.00×10^{-5}–8.00×10^{-4} mol/L CA. As the highest DIP I_p was attained for 2.00×10^{-4} mol/L CA (Figures S1 and S2), this concentration was further

kept constant, and the template concentration was changed from 1.00×10^{-5} mol/L to 1.60×10^{-4} mol/L DIP. In these conditions, the most intense DIP peak was reached when the polymerization mixture contained 4.00×10^{-5} mol/L DIP (Figure S2);

- The influence of the number of voltammetric potential cycles

The thickness of the polymeric film has a crucial role in its stability and conductivity, and, therefore, it must be optimized. Cyclic voltammetry offers the advantage of controlling the thickness of the MIP layer through the number of applied potential cycles. Further on, the influence of the number of potential cycles used in the electropolymerization stage on DIP anodic peak current was investigated (Figure S3), and the results showed that five voltammetric cycles were enough to obtain the highest DPV response for DIPat MIP_PGE;

- The influence of the scan rate

During the optimization step of the electropolymerization conditions, the influence of the scan rate was studied by varying it between 0.050–0.200 V/s while keeping constant the previously established parameters. The most intense DIP anodic peak was recorded when the electropolymerization was carried out with a scan rate of 0.100 V/s (Figure S4).

3.2.2. Optimization of the Conditions for Template Removal

The template molecules embedded in the polymer must be withdrawn from this matrix in order to create selective recognition sites. To ensure the optimal conditions for the elimination of the DIP molecules from the pCA skeleton, the PGE modified with the polymeric layer was kept in 96% ethanol for different time spans (10, 15, 30, 60, 90, and 120 min). The DIP removal was monitored by conducting DPV recordings in PBS pH = 7.00. The similar peak potential and shape of the signal obtained in PBS pH = 7.00 at PGE modified with pCA containing DIP in its matrix and at unmodified PGE in PBS pH = 7.00 containing DIP suggested that the DIP molecule retained in the polymeric matrix was not destroyed or changed. The DIP characteristic oxidation peak decreased with increasing immersion time and disappeared after 120 min, suggesting that the polymer film no longer contained template molecules. Similarly, various compositions of the extraction solution, namely, EtOH:PBS pH = 7.00 (1:1 v/v), EtOH:PBS pH = 7.00 (1:3 v/v), EtOH:PBS pH = 7.00 (3:1 v/v), and PBS pH = 7.00 were also tested, but they did not lead to shorter times for the complete template removal. Moreover, when the resulting electrodes were applied to DIP DPV analysis in PBS pH = 7.00, the pCA characteristic signal was absent, and the DIP peak height was similar to that recorded at bare PGE in the same working conditions. These observations led to the conclusion that most probably the polymeric film was destroyed after long maintenance in these media.

3.3. Electrode Surface Characterization

The electroactive areas of the bare PGE, NIP_PGE, and MIP_PGE were assessed by performing cyclic voltammetry recordings at various scan rates at each of the listed working electrodes in 1.00×10^{-4} mol/L $K_4Fe(CN)_6$ in 0.10 mol/L KCl solution and using the slopes of the regression equations of the I_p (A) = $f(v^{1/2}, (V/s)^{1/2})$ dependencies and the Randles–Sevcik equation I_p (A) = $2.95 \times 10^5 \times n^{3/2} \times A_{ea} \times D^{1/2} \times C_0 \times v^{1/2}$, where I_p (A) is the peak current; n is the number of transferred electrons(n = 1); A_{ea} (cm^2) is the electrode electroactive surface area; D (cm^2/s) is the diffusion coefficient of $K_4Fe(CN)_6$ in 0.1 mol/L KCl (D = 7.6×10^{-6} cm^2/s) [28]; v (V/s) is the scan rate, and C_0 (mol/cm^3) is the concentration of $K_4Fe(CN)_6$.

The obtained A_{ea} values were 0.0774 cm^2, 0.0777 cm^2, and 0.0816 cm^2 for bare PGE, NIP_PGE, and MIP_PGE, respectively. These results indicate only a slight increase (105.37%) in the MIP_PGE A_{ea} in comparison to that in the bare PGE. Therefore, the increase of 28% of the DIP oxidation signal and the shift of DIP peak potential toward lower values at MIP_PGE (0.386 V) vs. that recorded at the bare electrode (0.425 V) occurred not only because of the enhancement of the A_{ea} but due to the electrocatalytic effect of films formed

by electropolymerization of natural phenolic antioxidants, as in the case of CA and the corresponding pCA layer [29]. It is worth mentioning that in the case of NIP_PGE, the DIP anodic signal was shifted more toward less positive potentials so that it overlapped with that of the CA.

To characterize the charge transfer resistance (R_{ct}) of the bare and various modified PGEs, the EIS measurements were conducted in PBS pH = 7.00 in the presence of the redox couple ferro-ferricyanide. From the Nyquist plots (Figure 3), the highest value of R_{ct} (10.2 kΩ) was obtained for the bare PGE. The conductivity of modified PGEs was higher as indicated by their much lower R_{ct} values which were 1.96 kΩ for the electrode modified with pCA film (NIP_PGE), 2.11 kΩ for the PGE modified with pCA containing the template molecule (MIP + T_PGE), and 3.12 kΩ for the PGE modified with pCA after the template removing (MIP_PGE).
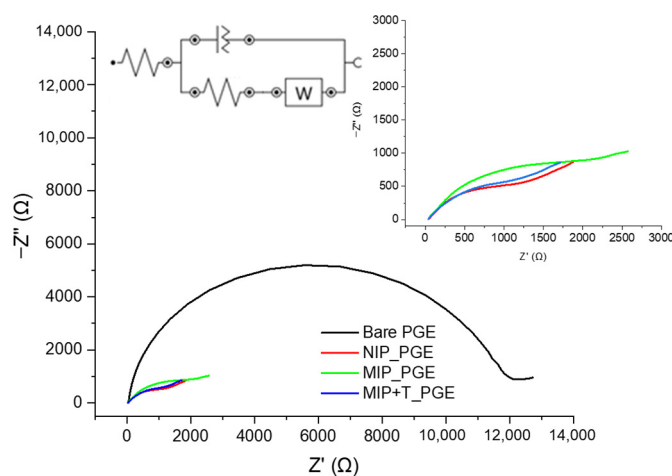
Figure 3. Impedance spectra recorded for bare PGE, NIP_PGE, MIP_PGE, and MIP + T_PGE in 1.00×10^{-3} mol/L $[Fe(CN)_6]^{4-}/[Fe(CN_6)]^{3-}$ in PBS pH = 7.00 at a DC potential of 0.230 V vs. Ag/AgCl and the equivalent circuit employed for the electrode's characterization. Inset: enlarged Nyquist plot of the NIP_PGE, MIP + T_PGE, and MIP_PGE.

NIP has the least resistance, indicating that pCA has the best conductivity among the tested modifiers deposited at the PGE. DIP presence in the polymer structure MIP+T led to a small increase in the Rct, the polymeric layer becoming somewhat less conductive, probably since DIP is less conductive than pCA sites. When the template was removed from the polymeric film, the formed cavities increased the resistance due to the return to the native PGE structure, which presented a higher resistance.

3.4. Voltammetric Analysis of DIP at MIP_PGE

3.4.1. The Influence of the Supporting Electrolyte pH on DIP Voltammetric Behavior at MIP_PGE

The electrochemical behavior of most electroactive organic compounds, especially those bearing ionizable groups, is influenced by the solution pH. Therefore, the voltammetric response of DIP at MIP_PGE was explored by both CV and DPV using as supporting electrolyte BRB solutions, with pH values ranging from 1.81 to 11.00. As one can observe from Figure 4a, regardless of the solution pH, if this was above 3.00, DIP cyclic voltammograms recorded at MIP_PGE showed only an anodic peak corresponding to the irreversible oxidation of the analyte. At pH = 1.81, the cyclic voltammograms presented two anodic and one cathodic signal; the anodic one, situated at about 0.620 V, responded to the analyte concentration and was attributed to DIP oxidation. The anodic and cathodic waves situated at less positive potentials corresponded to a reversible redox pair assigned to the CA electrode process, as these signals appeared also in the CVs recorded at MIP_PGE in the corresponding supporting electrolyte (Figure S5a). Because DPV is a more sensitive

technique in comparison to CV, the anodic peak corresponding to CA (Figure S5b) was observed in media with a pH of up to 4.00 (Figure 4b).

(a)   (b)
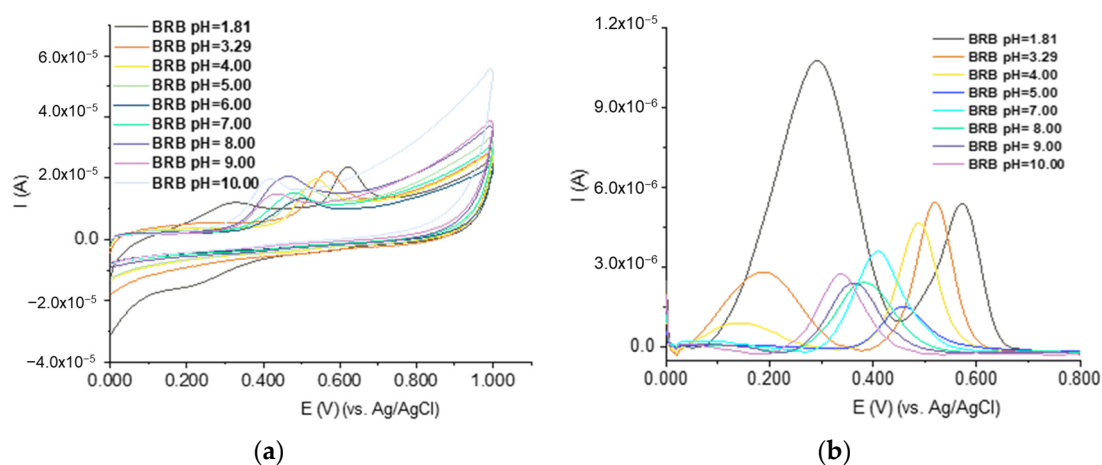
Figure 4. Cyclic (scan rate 0.100 V/s) (**a**) and differential pulse voltammograms (**b**) recorded at MIP_PGE for solutions of 5.00×10^{-5} mol/L DIP in BRB solutions with different pH values.

The potential of the DIP oxidation peak (E_p) became less positive when the solution pH increased due to the involvement of protons in the corresponding electrode process. The slopes of the regression equations $E_p = -0.02678 \times pH + 0.658$ ($R^2 = 0.99301$) and $E_p = -0.02812 \times pH + 0.60468$ ($R^2 = 0.97218$) for CV (Figure 5a) and DPV (Figure 5b), respectively, describing the $E_p = f$ (pH) dependencies, were close to half of the theoretical value given by the Nernst relation, suggesting that the ratio between the number of protons and the number of electrons participating in DIP electro-oxidation was $\frac{1}{2}$. This observation was in accordance with the data previously reported for the DIP electrode process at bare PGE [30].

(a)   (b)
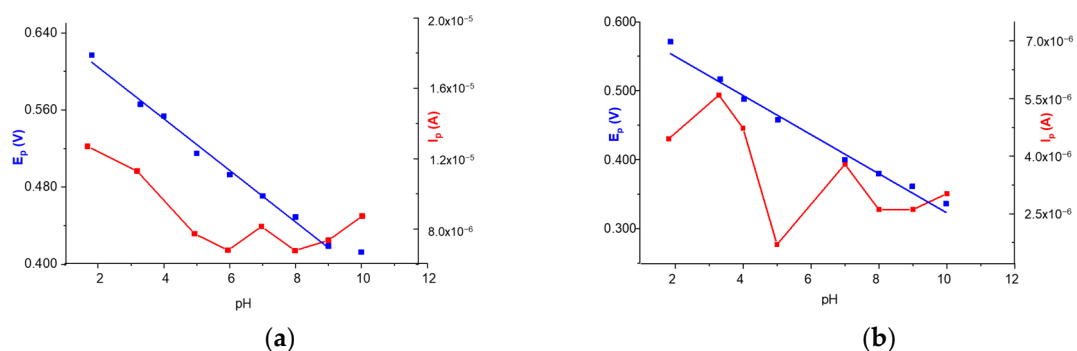
Figure 5. Variation of DIP oxidation peak potential and current with pH for CV (**a**) and DPV (**b**) analysis at MIP_PGE.

3.4.2. The Effect of the Potential Scan Rate on DIP Voltammetric Behavior at MIP_PGE

Cyclic voltammograms were conducted at different scan rates in order to elucidate the nature of the DIP electrode process at MIP_PGE. Despite the fact that the highest anodic peaks were obtained for DIP in acidic media, there was also a high interference from the pCA signal (Figure S5), so these environments were not further considered. Thus, the effect of the potential scan rate was investigated only in neutral solutions (Figure 6), where the next highest signals were obtained (Figure 5). Comparing the DPV signals obtained at MIP_PGE for DIP in PBS pH = 7.00 during the steps conducted for the optimization of the MIP formation at the PGE with those obtained in BRB pH = 7.00 for the same DIP concentration, it was observed that the higher ones were recorded in PBS pH = 7.00, and, therefore, this electrolyte was selected for further studies. This pH value was also suitable

as it was near to the physiological pH. CV recordings emphasized that DIP anodic signal was higher for faster scan rates and shifted toward more anodic potentials, this being characteristic of irreversible electrode processes. Considering the different dependencies of the DIP anodic peak currents on the potential scan rate (Table 1), it was concluded that DIP electro-oxidation at MIP_PGE was a mixed one, involving both diffusion and adsorption phenomena, but it was predominantly controlled by the diffusion of the analyte toward the electrode surface, due to the following facts: (i) the correlation coefficient of the $I_p = f(v^{1/2})$ dependence was higher than that of the $I_p = f(v)$ relation; and (ii) the slope of the regression equation describing the $\log I_p = f(\log v)$ variation was between 0.500 and 1.000 but closer to the theoretical value for a diffusion controlled process.
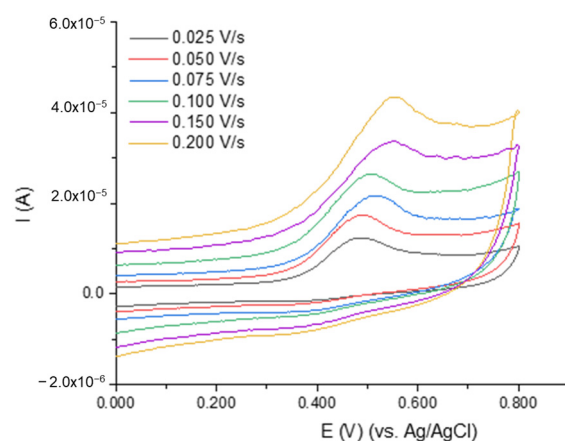
Figure 6. Cyclic voltammograms recorded at the MIP_PGE for 1.50×10^{-4} mol/L DIP in PBS pH = 7.00 at different scan rates.

Table 1. The regression equations for the different dependencies of the DIP anodic peak currents (I_p, A) on the potential scan rate (v, V/s).

Dependence	Regression Equation
$I_p = f(v)$	$I_p = 7.053 \times 10^{-5} \times v + 3.692$ ($R^2 = 0.9629$)
$I_p = f(v^{1/2})$	$I_p = 4.411 \times 10^{-5} \times v^{1/2} - 2.534 \times 10^{-6}$ ($R^2 = 0.996$)
$\log I_p = f(\log v)$	$\log I_p = 0.606 \times \log v - 4.338$ ($R^2 = 0.988$)

3.4.3. The Effect of DIP Concentration on Its Voltammetric Response at MIP_PGE

The variation of DIP oxidation peak intensity with the change in its concentration in the range of 1.00×10^{-7}–1.00×10^{-5} mol/L was investigated by DPV at the MIP_PGE in PBS pH = 7.00 (Figure 7). The linear variation of the oxidation peak current with DIP concentration corresponded to the regression equation I_p (A) = $0.902 \times C_{DIP}$ (mol/L) + 2.000×10^{-7} ($R^2 = 0.9943$), which was valid for the entire investigated concentration range.

To decrease the lower limit of the linear range obtained for the DPV determination of DIP at MIP_PGE, the accumulation of DIP at the electrode surface was investigated by applying an accumulation time (t_{acc}) of 10 s and changing the accumulation potential (E_{acc}) from -0.200 V to 0.200 V (Figure S6a). Since the DIP's highest peak current was recorded at an E_{acc} of 0.200 V, in the next step, this accumulation potential was applied to the MIP_PGE, and t_{acc} was gradually increased to 45 s. The DIP oxidation signal was enhanced with increasing t_{acc} until 30 s and slightly decreased for longer accumulation time spans (Figure S6b), most probably due to the saturation of the electrode surface with the analyte molecules.
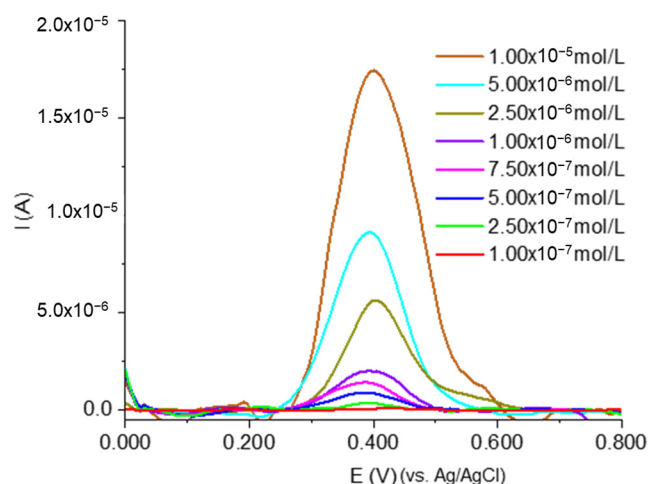
Figure 7. Differential pulse voltammograms recorded at the MIP_PGE for different DIP concentrations in PBS pH = 7.00.

Applying the adsorptive stripping voltammetric (Ads-DPV) technique under the optimized accumulation conditions at MIP_PGE, a linear dependence, described by the regression equation I_p (A) = $7.368 \times C_{DIP}$ (mol/L) + 8.193×10^{-8} (R^2 = 0.9964), was obtained between DIP anodic peak current and the analyte concentration in the range from 1.00×10^{-8} to 5.00×10^{-7} mol/L DIP (Figure 8).
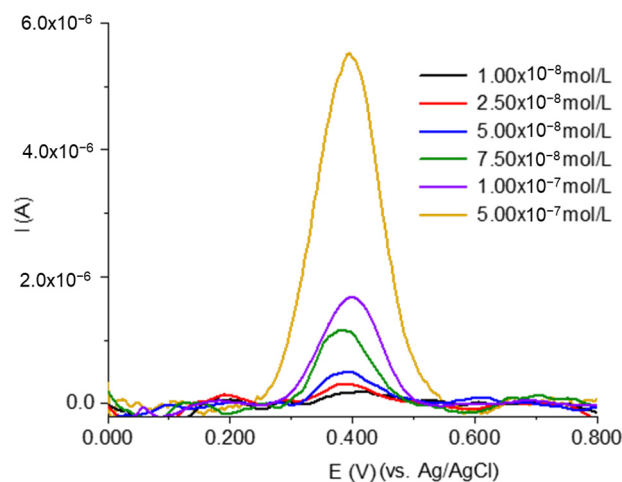
Figure 8. Adsorptive stripping differential pulse voltammograms recorded at MIP_PGE for different DIP concentrations in PBS pH = 7.00; t_{acc} = 30 s; E_{acc} = 0.200 V.

3.4.4. Limits of Detection and Quantification

The limits of detection (LOD) and quantification (LOQ) of the two methods developed for DIP quantification at MIP_PGE were calculated according to the relations $3.3 \times \sigma_{c,min}$ /S and LOQ = $10.0 \times \sigma_{c,min}$ /S, where $\sigma_{c,min}$ represents the standard deviation of the concentration corresponding to the lower limit of the linear range, and S is the slope of the regression equation describing the calibration curve [31]. The LOQ values were 6.80×10^{-8} mol/L DIP and 2.89×10^{-8} mol/L DIP for the DPV and AdS-DPV methods, respectively, while the values obtained for LOD are presented in Table 2. The performance characteristics presented by the MIP_PGE were comparable with those of other sensors presented in the literature. It must be emphasized that the previously reported MIP-based electrodes enabled the quantification of lower DIP concentrations than the MIP-PGE, but they also employed much longer accumulation/incubation times, namely 120 s [22] and 40 min [21], respectively.

Table 2. Performance characteristics of the electroanalytical methods presented in the literature for DIP quantification.

Electrode	Technique	Linear Range (mol/L)	LOD (mol/L)	Sample	Ref
HMDE	SWV	8.92×10^{-9}–4.99×10^{-6}	3.96×10^{-8}	Human serum	[32]
HMDE	SWV	1.29×10^{-7}–7.01×10^{-7}	1.88×10^{-6}	Tablets	[5]
CPE	DPV	5.94×10^{-5}–2.38×10^{-2}	1.98×10^{-5}	Tablets	[3]
Nafion-GCE	ASV	1.00×10^{-9}–8.00×10^{-8}	8.00×10^{-11}	Human serum	[33]
NiCo$_2$O$_4$/NiO@MOF-5/rGO/GCE	DPV	2.00×10^{-8}–5.50×10^{-4}	2.80×10^{-9}	Free-drug plasma, urine	[18]
BDDE	DPV	1.00×10^{-5}–5.00×10^{-6}	4.00×10^{-10}	Pharmaceuticals, human urine	[19]
SCPE	SWV	8.00×10^{-8}–3.00×10^{-5}	2.00×10^{-8}	Pharmaceuticals	[34]
PGE	DPV	5.00×10^{-7}–2.50×10^{-4}	1.21×10^{-7}	Tablets	[30]
MIP modified MGCE	DPV	9.91×10^{-10}–3.76×10^{-6}	5.95×10^{-11}	Human serum	[21]
MIP modified CPE	DPV	1.98×10^{-9}–2.18×10^{-7}	9.90×10^{-10}	Tablets, human serum	[22]
MIP_PGE	DPV	1.00×10^{-7}–1.00×10^{-5}	2.04×10^{-8}	Tablets	This work
	AdS-DPV	1.00×10^{-8}–5.00×10^{-7}	8.67×10^{-9}		

HMDE: Hanging Mercury Drop Electrode. CPE: Carbon Paste Electrode. GCE: Glassy Carbon Electrode. MOF: Metal–Organic Frameworks. rGO = reduced Graphene Oxide. BDDE: Boron-Doped Diamond Electrode. SCPE: Syringe Carbon Paste Electrode. MGCE: Magnetic Glassy Carbon Electrode. SWV: square wave voltammetry.

3.4.5. Repeatability

The repeatability of the DIP response recorded in PBS pH = 7.00 at MIP_PGE by DPV and AdS-DPV, expressed as relative standard deviation (RSD%) (Table 3), was evaluated at three concentration levels, namely, the lowest, an intermediate, and the highest concentrations of the corresponding linear range. The precision of the developed methods, expressed as relative standard deviation (RSD%), was assessed for each concentration from ten recordings always performed at a new MIP_PGE. The obtained RSD% values were within the limits accepted for each concentration level [35].

Table 3. Repeatability (precision) results of the DPV and AdS-DPV methods developed for DIP quantification at MIP-PGE in PBS pH = 7.00.

Technique	DPV			AdS-DPV		
DIP concentration (mol/L)	1.00×10^{-7}	1.00×10^{-6}	1.00×10^{-5}	1.00×10^{-8}	7.50×10^{-8}	5.00×10^{-7}
RSD %	9.98	4.82	4.50	5.93	5.52	2.44

3.4.6. Interferences

The DIP response at MIP_PGE was investigated in the presence of other biologically important compounds, such as urea, glucose, thiamine, ascorbic acid, and aspirin, at an analyte (1.00×10^{-6} mol/L) to interfering species (1.00×10^{-5} mol/L) concentration ratio of 1:10 (Figure 9). From all tested compounds; only urea presented a small anodic peak at cca. 0.090 V, with a peak current of about 5×10^{-7} A.

The tolerance limit was considered to be the maximum concentration of a substance that gave a ±10% signal change in the determination of 1.00×10^{-6} mol/L DIP. The experimental results emphasized that the DIP peak current increased by 4.76% in the presence of urea, while the other compounds generated a decrease in the DIP oxidation signal recorded at MIP_PGE. When DIP coexisted with a 10-fold higher concentration of glucose, thiamine, ascorbic acid, and aspirin, the changes in its peak current were 4.76%, 8.57%, 9.52%, and 0.95%, respectively.

3.4.7. Analytical Application of the Developed MIP-PGE for DIP Determination

The developed MIP_PGE was applied to the DIP quantification from pharmaceutical tablets by employing DPV in PBS pH = 7.00 and the standard addition method in order to minimize the matrix effects. The DPV curves of the working solution (dipyridamole tablet sample solution), always recorded at a new MIP_PGE, presented only the DIP characteristic anodic peak situated at about 0.400 V, suggesting that the tablet excipients were electro-inactive in the selected voltammetric conditions. The anodic peak currents

measured for the DIP signal obtained for the dipyridamole tablet sample solution before and after three successive additions of DIP standard solution (Figure 10a), as described in the Experimental section, increased linearly with increasing concentrations of DIP added (Figure 10b) and were used to assess the DIP content of the analyzed pharmaceutical sample, considering also the carried out dilutions. The results presented in Table 4 indicate the suitability of the developed DPV at the MIP_PGE method for DIP quantification from pharmaceutical samples.
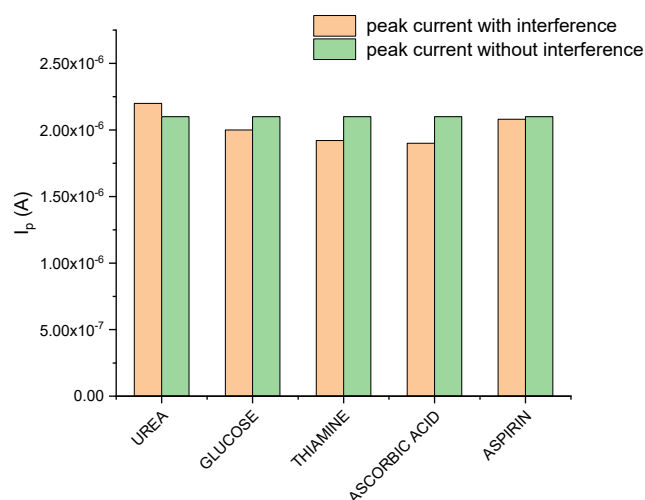
Figure 9. Comparison between the DIP peak currents recorded at MIP_PGE in the absence and in the presence of possible interfering biological important compounds.

(**a**)   (**b**)
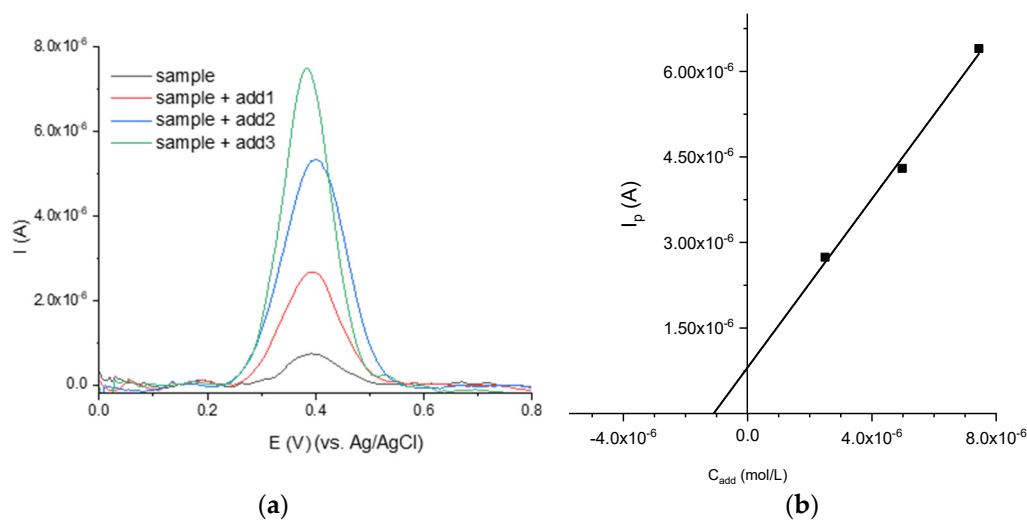
Figure 10. (**a**) Differential pulse voltammograms recorded at MIP_PGE for 10 mL dipyridamole tablet sample solution in PBS pH = 7.00, before and after each addition of 0.025 mL of 1.00×10^{-3} mol/L DIP stock solution; (**b**) the dependence of the peak current on the added DIP concentration.

Table 4. The results obtained for DIP determination from tablets using DPV at MIP-PGE in PBS pH = 7.00.

Tablet Content Claimed by the Producer (mg)	25.00
Tablet content found by DPV at MIP_PGE (mg) $\pm$ SD *	26.25 ± 0.25
RSD (%)	1.95
Recovery, R $\pm$ SD (%)	105.16 ± 0.02

* SD: standard deviation (n = 3).

4. Conclusions

This study presented DIP voltammetric behavior and its determination by using a disposable MIP_PGE. The modified working electrode was obtained by the rapid potentiodynamic electropolymerization of the non-toxic caffeic acid, a naturally occurring polyphenol, in the presence of the analyte molecule acting as a template using a cost-effective and commonly available PGE and DIP subsequent simple extraction in ethanol. Due to the pCA electrocatalytic effect and the accumulation of the analyte in the selective cavities of the MIP, the DIP irreversible, pH-dependent anodic signal was 28% higher at the MIP_PGE when compared with that generated by the bare PGE. Thus, DIP DPV analysis was more sensitive at the modified vs. bare PGE, but AdS-DPV was not as sensitive as that reported for the other MIP-modified sensors. However, the linear ranges of almost two orders of magnitude and the limits of detection situated at the tens nanomolar level of the DPV and AdS-DPV methods at the developed MIP_PGE are suitable for DIP quantification in pharmaceutical samples and in human blood plasma when one considers the DIP plasma levels between 0.800 and 2.32 μg/mL (1.58×10^{-6} to 4.60×10^{-6} mol/L) and of the tenfold lower DIP glucuronide levels reported by Dresse et al. [36], as well as the MIP_PGE's good selective behavior in the presence of common biologically important compounds. The recovery results from our study emphasized the MIP_PGE applicability for the DIP drug control analysis.

Conflicts of Interest: The authors declare no conflict of interest. The funders had no role in the design of the study, in the collection, analyses, or interpretation of data, in the writing of the manuscript, or in the decision to publish the results.

References

1. Lee, S.-D.; Huang, W.-C.; Peng, N.-J.; Hu, C. Dipyridamole-Induced Adverse Effects in Myocardial Perfusion Scans: Dynamic Evaluation. *IJC Heart Vasc.* **2016**, *14*, 14–19. [CrossRef] [PubMed]
2. Allahham, M.; Lerman, A.; Atar, D.; Birnbaum, Y. Why Not Dipyridamole: A Review of Current Guidelines and Re-Evaluation of Utility in the Modern Era. *Cardiovasc. Drugs Ther.* **2022**, *36*, 525–532. [CrossRef] [PubMed]
3. Li, C. Electrochemical Determination of Dipyridamole at a Carbon Paste Electrode Using Cetyltrimethyl Ammonium Bromide as Enhancing Element. *Colloids Surf. B Biointerfaces* **2007**, *55*, 77–83. [CrossRef] [PubMed]
4. Liu, X.; Li, Z.; Liu, S.; Sun, J.; Chen, Z.; Jiang, M.; Zhang, Q.; Wei, Y.; Wang, X.; Huang, Y.-Y.; et al. Potential Therapeutic Effects of Dipyridamole in the Severely Ill Patients with COVID-19. *Acta Pharm. Sin. B* **2020**, *10*, 1205–1215. [CrossRef]
5. De Toledo, R.A.; Castilho, M.; Mazo, L.H. Determination of Dipyridamole in Pharmaceutical Preparations Using Square Wave Voltammetry. *J. Pharm. Biomed. Anal.* **2005**, *36*, 1113–1117. [CrossRef]
6. Prakash, K.; Kalakuntla, R.R.; Sama, J.R. Rapid and Simultaneous Determination of Aspirin and Dipyridamole in Pharmaceutical Formulations by Reversed-Phase High Performance Liquid Chromatography (RP-HPLC) Method. *Afr. J. Pharm. Pharmacol.* **2011**, *5*, 244–251. [CrossRef]
7. Mallavarapu, R.; Katari, N.K.; Dongala, T.; Rekulapally, V.K.; Marisetti, V.M.; Vyas, G. A Validated Stability-Indicating Reversed-Phase-HPLC Method for Dipyridamole in the Presence of Degradation Products and its Process-Delated Impurities in Pharmaceutical Dosage Forms. *Biomed. Chromatogr.* **2022**, *36*, e5247. [CrossRef]
8. Rajput, A.P.; Sonanis, M.C. Development and Validation of a Rapid RP-UPLC Method for the Determination of Aspirin and Dipyridamole in Combined Capsule Formulation. *J. Appl. Pharm. Sci.* **2011**, *3*, 156–160.
9. Hammud, H.H.; El Yazbi, F.A.; Mahrous, M.E.; Sonji, G.M.; Sonji, N.M. Stability-Indicating Spectrofluorimetric and RP-HPLC Methods for the Determination of Aspirin and Dipyridamole in Their Combination. *Open Spectrosc. J.* **2008**, *2*, 19–28. [CrossRef]
10. Menaka, T.; Kuber, R. UPLC-Q-TOF-MS method development and validation for simultaneous analysis of dipyridamole and its related impurities. *J. Appl. Pharm. Sci.* **2023**, *13*, 201–211. [CrossRef]
11. Barghash, S.; Abd El-Razeq, S.; El -Awady, M.; Belal, F. Validated Spectrophotometric Method for Analysis of Dipyridamole and Lamivudine Using Eosin Y. *Azhar IJPSM* **2021**, *1*, 73–82. [CrossRef]
12. Sushama, R.A.; Jayesh, P.T.; Vijay, A.B. Development and Validation of Simple and Rapid UV Spectroscopic Method for Estimation of Dipyridamole in Tablet Dosage Form. *IOSR J. Appl. Chem.* **2021**, *14*, 14–22. [CrossRef]
13. Serebruany, V.; Pokov, I.; Hanley, D. Spectrofluorimetric Assessment of Plasma Dipyridamole Stability: Sample Storage for Multicenter Clinical Trials? *Thromb. Res.* **2008**, *123*, 184–186. [CrossRef]
14. Wang, L.; Tang, Y. Determination of Dipyridamole using TCPO–H_2O_2 Chemiluminescence in the Presence of Silver Nanoparticles. *Luminescence* **2011**, *26*, 703–709. [CrossRef]
15. Fahelelbom, K.M.S.; El-Shabrawy, Y. Simultaneous Determination of Dipyridamole and Acetylsalicylic Acid in Pharmaceuticals and Biological Fluids by Synchronous and First Derivative Synchronous Fluorimetry. *J. Pharm. Sci. Res.* **2019**, *11*, 2949–2955.
16. Ankitha, M.; Shabana, N.; Rasheed, P.A. A Novel ReS2–Nb2CTx Composite as a Sensing Platform for Ultrasensitive and Selective Electrochemical Detection of Dipyramidole from Human Serum. *Graphene 2D Mater.* **2022**, *8*, 27–37. [CrossRef]
17. Afkhami, A.; Moosavi, R.; Madrakian, T. Maghemite-Nanoparticles Enhanced Effects in Electrochemical Determination of Dipyridamole Utilizing Simultaneous Statistical Based Experimental Design Optimization. *J. Electrochem. Soc.* **2013**, *160*, H775–H781. [CrossRef]
18. Salandari-Jolge, N.; Ensafi, A.A.; Rezaei, B. Metal–Organic Framework Derived Metal Oxide/Reduced Graphene Oxide Nanocomposite, a New Tool for the Determination of Dipyridamole. *N. J. Chem.* **2021**, *45*, 2781–2790. [CrossRef]
19. Sarakhman, O.; Pysarevska, S.; Dubenska, L.; Stanković, D.M.; Otřísal, P.; Planková, A.; Kianičková, K.; Švorc, Ľ. Voltammetric Protocol for Reliable Determination of a Platelet Aggregation Inhibitor Dipyridamole on a Bare Miniaturized Boron-Doped Diamond Electrochemical Sensor. *J. Electrochem. Soc.* **2019**, *166*, B219–B226. [CrossRef]
20. Preda, D.; David, I.G.; Popa, D.E.; Buleandra, M.; Radu, G.L. Recent Trends in the Development of Carbon-Based Electrodes Modified with Molecularly Imprinted Polymers for Antibiotic Electroanalysis. *Chemosensors* **2022**, *10*, 243. [CrossRef]
21. Liu, X.; Zhong, J.; Rao, H.; Lu, Z.; Ge, H.; Chen, B.; Zou, P.; Wang, X.; He, H.; Zeng, X. Electrochemical Dipyridamole Sensor Based on Molecularly Imprinted Polymer on Electrode Modified with Fe3O4@Au/Amine-Multi-Walled Carbon Nanotubes. *J. Solid State Electrochem.* **2017**, *21*, 3071–3082. [CrossRef]

22. Javanbakht, M.; Fathollahi, F.; Divsar, F.; Ganjali, M.R.; Norouzi, P. A Selective and Sensitive Voltammetric Sensor Based on Molecularly Imprinted Polymer for the Determination of Dipyridamole in Pharmaceuticals and Biological Fluids. *Sens. Actuators B Chem.* **2013**, *182*, 362–367. [CrossRef]

23. David, I.G.; Litescu, S.C.; Popa, D.E.; Buleandra, M.; Iordache, L.; Albu, C.; Alecu, A.; Penu, R.L. Voltammetric Analysis of Naringenin at a Disposable Pencil Graphite Electrode—Application to Polyphenol Content Determination in Citrus Juice. *Anal. Methods* **2018**, *10*, 5763–5772. [CrossRef]

24. Nian, B.L.; Ren, W.; Hong, Q.L. Caffeic Acid-Modified Glassy Carbon Electrode for the Simultaneous Determination of Epinephrine and Dopamine. *Electroanalysis* **2007**, *19*, 1496–1502. [CrossRef]

25. Lee, P.T.; Ward, K.R.; Tschulik, K.; Chapman, G.; Compton, R.G. Electrochemical Detection of Glutathione Using a Poly(Caffeic Acid) Nanocarbon Composite Modified Electrode. *Electroanalysis* **2014**, *26*, 366–373. [CrossRef]

26. Rohanifar, A.; Devasurendra, A.M.; Young, J.A.; Kirchhoff, J.R. Determination of L-DOPA at an Optimized Poly(Caffeic Acid) Modified Glassy Carbon Electrode. *Anal. Methods* **2016**, *8*, 7891–7897. [CrossRef]

27. Li, R.; Zhai, T.; Zhao, L.; Zhang, N.; He, M.; Tan, L. Preparation of Poly(caffeic acid)-CoP Nanoparticle Film on Electrode Surface and Sensitive Voltammetric Detection of Acetaminophen. *Colloids Surf. A Physicochem. Eng. Asp.* **2021**, *627*, 127173. [CrossRef]

28. Konopka, S.J.; McDuffie, B. Diffusion Coefficients of Ferri- and Ferrocyanide Ions in Aqueous Media, Using Twin-Electrode Thin-Layer Electrochemistry. *Anal. Chem.* **1970**, *42*, 1741–1746. [CrossRef]

29. Ziyatdinova, G.; Guss, E.; Yakupova, E. Electrochemical Sensors Based on the Electropolymerized Natural Phenolic Antioxidants and Their Analytical Application. *Sensors* **2021**, *21*, 8385. [CrossRef]

30. David, I.G.; Iordache, L.; Popa, D.E.; Buleandra, M.; David, V.; Iorgulescu, E.E. Novel Voltammetric Investigation of Dipyridamole at a Disposable Pencil Graphite Electrode. *Turk J. Chem.* **2019**, *43*, 1109–1122. [CrossRef]

31. Miller, J.N.; Miller, J.C. *Statistics and Chemometrics for Analytical Chemistry*, 6th ed.; Pearson: London, UK, 2010; ISBN 978-0-273-73042-2.

32. Ghoneim, M.M.; Tawfik, A.; Radi, A. Assay of Dipyridamole in Human Serum Using Cathodic Adsorptive Square-Wave Stripping Voltammetry. *Anal. Bioanal. Chem.* **2002**, *374*, 289–293. [CrossRef] [PubMed]

33. Wang, Z.; Zhang, H.; Zhou, S. Determination of Trace Amounts of Dipyridamole by Stripping Voltammetry Using a Nafion Modified Electrode. *Talanta* **1997**, *44*, 621–626. [CrossRef] [PubMed]

34. Yari, A.; Shams, A. Fabrication of a Renewable Syringe Carbon Paste Electrode with a Motor Rotary Blade and Using for Voltammetric Measurement of Dipyridamole. *J. Iran Chem. Soc.* **2018**, *15*, 1861–1869. [CrossRef]

35. AOAC International. Guidelines for Standard Method Performance Requirements. Available online: https://www.aoac.org/wp-content/uploads/2019/08/app_f.pdf (accessed on 25 May 2023).

36. Dresse, A.; Chevolet, C.; Delapierre, D.; Masset, H.; Weisenberger, H.; Bozler, G.; Heinzel, G. Pharmacokinetics of Oral Dipyridamole (Persantine®) and Its Effect on Platelet Adenosine Uptake in Man. *Eur. J. Clin. Pharmacol.* **1982**, *23*, 229–234. [CrossRef] [PubMed]